

# Resource-dependent heterosynaptic spike-timing-dependent plasticity in recurrent networks with and without synaptic degeneration

James Humble<sup>1</sup>

<sup>1</sup> Randolph, MA, USA

Correspondence\*:

James Humble

james.m.d.humble@gmail.com

2 Number of words: 3295

3 Number of figures: 4

4 Number of tables: 0

## 5 ABSTRACT

6 Many computational models that incorporate spike-timing-dependent plasticity (STDP) have  
7 shown the ability to learn from stimuli, supporting theories that STDP is a sufficient basis  
8 for learning and memory. However, to prevent runaway activity and potentiation, particularly  
9 within recurrent networks, additional global mechanisms are commonly necessary. A STDP-  
10 based learning rule, which involves local resource-dependent potentiation and heterosynaptic  
11 depression, is shown to enable stable learning in recurrent spiking networks. A balance between  
12 potentiation and depression facilitates synaptic homeostasis, and learned synaptic characteristics  
13 align with experimental observations. Furthermore, this resource-based STDP learning rule  
14 demonstrates an innate compensatory mechanism for synaptic degeneration.

15 **Keywords:** spike-timing-dependent plasticity, homeostasis, heterosynaptic, recurrent network, learning, spiking, synaptic  
16 degeneration, neurodegeneration

## 1 INTRODUCTION

17 The concept of spike-timing-dependent plasticity (STDP) has been thoroughly researched and frequently  
18 serves as a foundation for learning in computational models. Various studies adopt STDP in diverse formats.  
19 For instance, it may be utilized with either an additive or a multiplicative rule for updates: Potentiation  
20 or depression may depend on or be independent of a synapse's weight. Different STDP implementations  
21 can lead to varied outcomes, with some rules more closely reflecting phenomena observed in experiments.  
22 These variations include 1) synaptic weight distributions, 2) the presence of nonpotentiable synapses, 3)  
23 silent synapses, 4) synaptic persistence, and 5) competition between synapses:

24 1. Empirically identified synaptic weight distributions generally display a uni-modal pattern that peaks  
25 close to zero, characterized by numerous weak synapses and a few strong connections forming a  
26 long tail (Buzsáki, 2004; Yasumatsu et al., 2008; Kasai, 2023). In computational models, synaptic

distributions change based on whether STDP is implemented additively or multiplicatively. In feedforward networks, additive STDP often produces bi-modal distributions, with peaks located near zero and the upper limit of synaptic weight (Rossum et al., 2000; Barbour et al., 2007; Morrison et al., 2008). In contrast, multiplicative STDP often generates uni-modal distributions with a peak situated between zero and the upper bound (Rossum et al., 2000; Barbour et al., 2007; Morrison et al., 2008). In recurrent networks, additive STDP can produce a uni-modal distribution with a peak at the upper-bound and multiplicative, uni- or multi-modal distributions (Morrison et al., 2007).

- 27
  - 28
  - 29
  - 30
  - 31
  - 32
  - 33
  - 34
  - 35
  - 36
  - 37
  - 38
  - 39
  - 40
  - 41
  - 42
  - 43
  - 44
  - 45
  - 46
  - 47
  - 48
  - 49
  - 50
  - 51
  - 52
  - 53
  - 54
  - 55
  - 56
  - 57
  - 58
  - 59
  - 60
  - 61
  - 62
  - 63
  - 64
  - 65
  - 66
  - 67
  - 68
  - 69
2. Silent synapses are primarily defined by their absence of  $\alpha$ -amino-3-hydroxy-5-methyl-4-isoxazolepropionic acid (AMPA) receptors, as comprehensively discussed by Montgomery and colleagues (2004). Despite the scarcity of AMPA receptors, these synapses often retain a degree of plasticity due to the presence of *N*-methyl-D-aspartate (NMDA) receptors (Kim et al., 2025). In a study by Brunel et al. (2004), a prominent and sharply delineated subset of silent synapses was integrated into an empirically derived distribution by assessing those potentially undetected because of technological limitations and their deficiency in AMPA receptors. Such a peak is observed in spine volume (Yasumatsu et al., 2008) and synaptic efficacy (Barbour et al., 2007).
3. Research has indicated that certain synapses may not be capable of potentiation. For instance, Debanne et al. (1999) reported the inability to induce potentiation in 24 % of the synapses examined. Debanne and colleagues propose that this nonpotentiability might be attributed to synapses individually reaching saturation. Conversely, computational models often employ either a universal upper limit across all synapses or a global normalizing mechanism and neglecting these constraints may lead to excessive activity and potentiation (Rossum et al., 2000).
4. The persistence of synapses is typically considered to be fundamentally important for memory. In their study, Billings et al. (2009) investigated the durability of synaptic weights governed by STDP principles and found that additive STDP facilitates stability, whereas multiplicative STDP causes instability due to rapid weight variations. Empirical evidence from long-term potentiation (LTP) studies indicates a two-phase persistence: an initial phase that diminishes swiftly and seems to be reliant on neuronal activity (Dong et al., 2015), and a later phase capable of sustaining LTP over prolonged periods, possibly extending to a year (Abraham et al., 2002). There is, however, strong evidence demonstrating that spine volumes fluctuate in the absence of activity and plasticity (reviewed by Kasai (2023)) and that such fluctuations combined with STDP can be stable (Humble et al., 2019). In this case, the mean spine volume of a group of neurons must be persistent rather than the individual synaptic strengths.
5. Whereas STDP following an additive rule is known for its strong competitive interactions, STDP governed by a multiplicative rule typically exhibits limited competition, prompting the incorporation of supplementary mechanisms such as synaptic scaling or intrinsic fluctuations to achieve the competition essential for learning (Rossum et al., 2000; Humble et al., 2019). The inherently competitive aspect of additive STDP typically necessitates enforcing a stringent upper limit on synaptic strength to control excessive potentiation. In contrast, multiplicative STDP operates under more flexible upper limits determined by weight dependency. A drawback of deploying global limits is their assignment of preset values before the learning process, which may not align with biological realism. Moreover, as mentioned above, Debanne et al. (1999) demonstrated the possibility of individual synaptic upper limits.

Furthermore, to control runaway activity, mechanisms such as synaptic scaling (Turrigiano, 2008), inhibition (Bannon et al., 2020; Eckmann et al., 2024), or the Beinenstock-Cooper-Munro rule (Cooper

70 and Bear, 2012) are typically included with Hebbian-based learning rules in recurrent networks. However,  
 71 these can operate on a slower timescale than STDP.

72 The above picture is further complicated by experiments showing that heterosynaptic plasticity can  
 73 occur at unstimulated spines near a stimulated one (reviewed by Chater and Goda (2021)). Essentially,  
 74 given some homosynaptic activity in a subset of spines, heterosynaptic changes have been observed at  
 75 unstimulated ones. The distance dependence and direction of these heterosynaptic changes are potentially  
 76 competitive (Chater et al., 2024).

77 Motivated by these experimental results, this paper explores ongoing research into computational  
 78 disparities by utilizing a learning methodology that integrates ‘resources’ alongside heterosynaptic plasticity  
 79 in a spiking recurrent network. In a computational model of individual neurons (Chen et al., 2013) and  
 80 a feedforward network (Chapter 5 of (Humble, 2013)), it has previously been shown that heterosynaptic  
 81 plasticity can be beneficial in controlling activity and plasticity.

82 In addition to networks with static connectivity, progressive loss of synapses is a hallmark of many  
 83 neurodegenerative diseases, including Huntington’s, Parkinson’s, and Alzheimer’s (Herms and Dorostkar,  
 84 2015; Meftah and Gan, 2023), and neuropsychiatric disorders such as schizophrenia and depression (Penzes  
 85 et al., 2011). To counteract synaptic loss, the existence of compensatory mechanisms has been suggested  
 86 that include enlargement of the remaining spines and increased spinogenesis (Bhembre et al., 2023).

87 By advancing STDP through the incorporation of limited resources for potentiation and merging it with  
 88 heterosynaptic depression that affects neighboring synapses, the results reveal that this model effectively  
 89 resolves the discrepancies mentioned above while presenting an innate mechanism for both synaptic  
 90 homeostasis and synaptic degeneration compensation.

## 2 METHODS

91 The network structure, Fig. 1a, consists of a pool of  $N_{\text{exc}} = 200$  excitatory neurons recurrently connected  
 92 with plastic excitatory synapses with a probability of 25 %. Independent Poisson spike trains are presented  
 93 to the pool with an input connection probability of 10 % from  $N_{\text{in}} = 50$  spike trains. All connections have  
 94 axonal delays drawn from a uniform distribution from 1 ms to 5 ms (Lemaréchal et al., 2021).

95 Excitatory neurons are refractory leaky integrate-and-fire cells, Eqs. 1. The membrane potential of each  
 96 neuron,  $v$ , follows low-pass dynamics with a time constant  $\tau_v = 25$  ms (Rall, 1969) and is reset when it  
 97 reaches the firing threshold,  $\theta = 1$ , Fig. 1b bottom.

$$\tau_v \frac{dv}{dt} = -v + r \left( \sum_i^{N_{\text{in}}} s_i + \sum_j^{N_{\text{exc}}} s_j \right) \quad (1a)$$

$$V \rightarrow 0 \quad \text{if } V \geq \theta \quad (1b)$$

98

99 An absolute refractory period of 3 ms is followed by a relative refractoriness period,  $\tau_r = 5$  ms, Eq. 2  
 100 and Fig. 1b middle.

$$\tau_r \frac{dr}{dt} = 1 - r \quad (2)$$

101 All input and recurrent afferents were modeled as synaptic currents,  $s'$  and  $s$ , Eqs. 3 and Fig. 1b top.  
 102  $\tau_{sr} = 2.6$  ms is the time constant for the synaptic current rise and  $\tau_{sf} = 31.3$  ms the decay constant (Hunt  
 103 et al., 2022). The input of each synapse consists of binary neuron spikes,  $I_i$ , scaled by the synapse's weight,  
 104  $w_i$ .

$$\tau_{sr} \frac{ds'}{dt} = -s' + I w \quad (3a)$$

$$\tau_{sf} \frac{ds}{dt} = -s + s' \quad (3b)$$

105 Pairs of presynaptic and postsynaptic spikes evoke changes in synaptic weight,  $\Delta w = f(\tau)$ , given as a  
 106 function of their temporal distance,  $\tau = \text{post-spike time} - \text{pre-spike time}$ , Fig. 1c. Equation 4 describes  
 107 the STDP function used, where  $\tau_{STDP} = 20$  ms (Bi and Poo, 1998). Depression is weight dependent,  
 108 as observed by Bi and Poo (1998), Fig. 1d. Recurrent weights were bounded  $[0, +\infty)$ . See below for a  
 109 description of the inclusion of 0.18 in depression.

$$f(\tau) = \begin{cases} \exp\left(\frac{-\tau}{\tau_{STDP}}\right) & \text{if } \tau \geq 0 \\ 0.18 \exp\left(\frac{\tau}{\tau_{STDP}}\right) w & \text{if } \tau < 0 \end{cases} \quad (4)$$

110 The initial input weights are set with random values drawn from a uniform distribution between 0 and 1.  
 111 All recurrent weights,  $w$ , are initially assigned 0 as akin to a newly formed network.

112 This typical STDP implementation is extended as in Humble (2013) to include the requirement of  
 113 resources for potentiation paired with potentiation-driven heterosynaptic depression in neighboring  
 114 synapses. Firstly, a pool of resources is included,  $p$ . Similarly to many receptors and proteins that undergo  
 115 degradation or recycling, the pool's resources decay with a time constant of  $\tau_p = 10$  s, Eq. 5.

$$\tau_p \frac{dp}{dt} = -p \quad (5)$$

116 The amounts of the initial resource pool are assigned by Eq. 6 where  $\xi$  is a random number from a  
 117 standard normal distribution. The constant multiple was found through a parameter search to ensure that the  
 118 weights were strong enough that the activity continued after stimulation stopped. A lognormal distribution  
 119 is chosen as skewed distributions are observed for many aspects of brain dynamics (Buzsáki and Mizuseki,  
 120 2014).

$$2 e^\xi \quad (6)$$

121 When updating the weights with resource-dependent STDP, there are three scenarios, Fig. 1e:

- 122 • When potentiating a synapse, its neighbors are actively depressed by an exponential function of their  
123 distance to the potentiating synapse, and the potentiating amount to a maximum distance of 3 synapses.  
124 • When a potentiating synapse and its neighbors have no resources left, the potentiating synapse acquires  
125 resources from the pool, if available.  
126 • When a synapse is depressed, its resources are relocated to the pool for reuse.
- 127 For simplicity, time constants for resource mobility are neglected; hence, resources can transfer between  
128 a synapse and the pool, and vice versa, within a single time step.
- 129 With local heterosynaptic plasticity, depression dominates because potentiation events are accompanied  
130 by depression, and thus depression has to be decreased. It has previously been found that 0.18 was a  
131 suitable multiple for depression such that potentiation and depression were balanced (Humble, 2013). This  
132 reduced depression, Fig. 1c, matches the experimental observations of decreased depression relative to  
133 potentiation (Bi and Poo, 1998).
- 134 The rate of the input spike trains is 50 Hz for the first 20 s, Fig. 1f.
- 135 All simulations used forward Euler integration with a time step of  $dt = 0.1$  ms and were implemented in  
136 MATLAB.

### 3 RESULTS

- 137 During stimulation of a typical network, most neurons in the excitatory pool fire with increased firing  
138 rates, Figs. 2a and 2b. After stimulation, a subset continues to fire representing a learned memory. Not all  
139 neurons are recruited into the memory, due to initial random input and recurrent connectivity and random  
140 activity-driven plasticity. Furthermore, after learning, the firing rates of many neurons change, Fig. 2c;  
141 nevertheless, the memory is preserved.
- 142 After learning, weight statistics match those found experimentally—five observations were identified in  
143 the introduction:
- 144 1. The weight distribution for recurrent connections at the end of the simulation is unimodal, Fig. 2d,  
145 matching those observed experimentally (see supplementary materials Fig. 1 for additive and  
146 multiplicative STDP results in this model.)
  - 147 2. The distribution also shows a large peak of empty synapses: silent synapses.
  - 148 3. Resource-based STDP endows reduced and nonpotentiability, Fig. 2e. Specifically, the actual  
149 potentiation amount as a percentage of that determined by the STDP window function demonstrates  
150 that sometimes not enough resources are available to fully potentiate a synapse; some times very little  
151 or no potentiation was observed.
  - 152 4. Resource-based STDP is stable, with weights remaining persistent in a longer simulation, Fig. 3.
  - 153 5. Weights converge to individual upper bounds despite the positive feedback loop present due to plasticity.  
154 It was observed that weights reach their own saturation points, Fig. 2f. Furthermore, due to the distance  
155 dependence of heterosynaptic depression, analysis indicates that resource-based heterosynaptic STDP  
156 promotes synaptic sparsity and synaptic competition for limited resources, with functional spines  
157 becoming spatially distributed along the dendrite. The average distance between a nonfilopodia spine  
158 and its nearest nonfilopodia spine neighbor increases during learning, Fig. 2g.

159 Most of the resources available in the neurons' pools quickly decrease due to plasticity driven changes,  
160 Fig. 2h. Some pools may not be used up due to plasticity and instead naturally decay.

161 During the initial learning phase, the network's in/out degree increases and stabilizes  $\approx 3$ , and the  
162 closeness (where the length of the paths is the axonal delay) decreases, Fig. 2i. The decrease in closeness  
163 demonstrates that learning optimizes for short delays.

164 After the initial learning phase, the network is further optimized with an increase in nonfilopodia spine  
165 distance and a decrease in closeness. Furthermore, the network structure changes during this optimization  
166 phase with weights increasing or decreasing, Figs. 2j to 2l. Most strong connections are stable with a few  
167 changing; the majority of optimization changes are with weaker synapses.

168 These results in a typical network demonstrate that resource-based STDP is capable of stable learning in  
169 recurrent networks with an innate homeostasis mechanism controlling runaway activity and potentiation.  
170 Next, to model spine loss in neurodegenerative diseases, synapses are progressively removed, Figs. 4a and  
171 4b.

172 In a typical network with resource-based heterosynaptic STDP, the memory is maintained until  $\approx 17\%$   
173 of the original connections remain, Fig. 4c. As synapses are removed, their resources replenish the pool and  
174 allow further compensatory potentiation with an increase in mean synaptic weight and transient increases  
175 in the pool of resources, Figs. 4d and 4e. However, when this replenishment is blocked, the memory is only  
176 maintained until  $\approx 72\%$  synapses remain, Fig. 4f—with no increase in the remaining synaptic weights,  
177 Fig. 4g.

178 This is further illustrated when comparing the sum of weights as a percentage of the maximum sum,  
179 Fig. 4h. Under the replenishment-blocking condition, the total synaptic input disappears  $\approx 4$  times faster  
180 than under the control condition. Moreover, loss of neuron activity is sudden without replenishment of  
181 resources; whereas with replenishment of resources there is a progressive loss, Fig. 4i.

## 4 DISCUSSION

182 Discrepancies were reconciled between computational STDP models and empirical observations by using  
183 a STDP framework based on resource-dependent heterosynaptic STDP in a recurrent spiking network. By  
184 integrating resource-dependent potentiation with heterosynaptic depression at nearby synapses, neurons  
185 performed a learning task while preserving synaptic weight attributes and statistical traits consistent with  
186 biological data.

187 Resource-dependent heterosynaptic STDP results in weight distributions characterized by a singular peak  
188 and a pronounced tail. The distribution also shows a large peak at zero of spines empty of resources (silent  
189 synapses) similar to those estimated by Brunel et al. (2004) and similar to an abundance of filopodia as  
190 seen by Yasumatsu et al. (2008) and reviewed by Kasai (2023).

191 Furthermore, this approach to heterosynaptic STDP incorporates robust competitive dynamics and  
192 synaptic homeostasis, leading to varying intrinsic upper limits for individual synapses at which a synapse  
193 is no longer potentiable. In addition, the STDP rule promotes sparse spatial encoding in afferents and  
194 therefore strong competition between neighboring spines for limited resources. This homeostasis among  
195 weights is independent of any additional normalization mechanism or universal constraints to regulate  
196 learning. Such synaptic homeostasis is a compelling mechanism for stabilizing neural activity and plasticity  
197 within recurrent networks.

Finally, given progressive synaptic loss, resource-based STDP demonstrated an innate compensatory mechanism due to replenishment of resources; this mechanism has been hypothesized to counteract a loss in input (Bhembre et al., 2023). Loss of synaptic input is associated with early stages of neurodegenerative diseases, for example, Alzheimer's disease (Spires et al., 2005). Resource-based STDP demonstrated the ability to maintain total synaptic input by replenishing resources in the pool after synaptic removal. Moreover, resource-based STDP demonstrated a sufficient substrate for observations showing enlargement of synapses following insults such as deafferentation and sensory deprivation (Chen and Hillman, 1982; Barnes et al., 2017) and the hypothesized spine enlargement in Alzheimer's disease (Bhembre et al., 2023). Finally, resource-based STDP exhibited a progressive loss in, rather than a sudden loss in, neuron activity. How this relates to aberrant activity observed in Alzheimer's disease (Korzhova et al., 2021) is unknown, and exploring this offers an interesting future extension to this work.

Given that the proposed STDP rule aligns with experimentally observed weight statistics and supports a hypothesized neurodegenerative compensatory mechanism, its potential biological plausibility warrants examination. Royer et al. (2003) observed in amygdala slices that the induction of long-term depression (potentiation) resulted in corresponding long-term potentiation (depression) at distally located dendritic sites, determined by the distance from the initial induction site. In contrast, Hou et al. (2008) reported no such synaptic changes at adjacent sites in cultured hippocampal neurons derived from rat embryos.

The research carried out by Oh et al. (2015) in P6-P7 hippocampal slice cultures aligns with the proposed STDP model. Stimulation-induced potentiation in specific spines was demonstrated to cause a reduction in the size of adjacent unstimulated spines. This observation can be explained by two potential mechanisms: first, the competition among nearby spines for a scarce resource, or second, an activity-triggered signal facilitating the reduction of adjacent spines. The findings of Oh et al. lend credence to the second hypothesis. They determined that blocking calcineurin, IP<sub>3</sub> receptors or group I metabotropic glutamate receptors hinders heterosynaptic shrinkage, without affecting the potentiation process when Ca<sup>2+</sup>/calmodulin-dependent protein kinase II (CaMKII) is inhibited. This evidence indicates that synaptic potentiation and the associated decrease in nearby synaptic strength operate through distinct pathways.

Bian et al. (2015) observed that competition among spines for cadherin/catenin complexes plays a crucial role in orchestrating both the maturation of individual spines and the pruning of adjacent spines. Their *in vivo* studies revealed that variations in cadherin/catenin complex concentrations between neighboring spines lead to a redistribution of β-catenin, which in turn influences whether a spine matures or is trimmed. Crucially, they demonstrated that this process depends on neuronal activity and the distance between the enlarging spine and the nearby one that is slated to be eliminated. Furthermore, this competitive mechanism was not limited to individual neurons; it occurred in neighboring neurons receiving similar axonal input.

Within the framework of long-term potentiation (LTP), the relocation of AMPA receptors to synaptic sites is associated with increased synaptic activity (Hayashi et al., 2000; Sutton and Schuman, 2006; Shi et al., 2001). In this process, CaMKII experiences autophosphorylation when intracellular Ca<sup>2+</sup> levels rise through NMDA receptor-mediated channels, culminating in the phosphorylation of GluR1 (Roche et al., 1996). AMPA receptors can originate from multiple sources, such as recycling endosomes (Park et al., 2004) and the trans-Golgi network (Horton and Ehlers, 2004). Our model consolidates these different origins into a common pool, taking advantage of evidence that AMPA receptors can traverse long distances, facilitated by movement along dendritic membranes (Choquet and Triller, 2003) and microtubule pathways (Washbourne et al., 2002). Regarding the mechanism that underlies heterosynaptic depression, Oh et al. (2015) observed that blocking calcineurin, IP<sub>3</sub>Rs, or group I metabotropic glutamate receptors hindered the contraction of adjacent spines. Additionally, Bian et al. (2015) propose the existence of a single molecular

242 structure that fulfills dual roles, both as a ‘resource’ and as a transmitter of depressive signals. Finally, recent  
243 experimental and computational evidence suggests that  $\text{Ca}^{2+}$  activity is a key component of competitive  
244 heterosynaptic plasticity (Chater et al., 2024).

245 The depiction of STDP herein does not include explicit modeling of biological signaling pathways or  
246 diffusible molecules that might cause depression in neighboring synapses after activity-driven potentiation,  
247 nor does it specify a precise timeline for such processes. Furthermore, it does not incorporate the transfer  
248 of resources into or out of a dendritic spine. Introducing these complexities could impose interesting  
249 limitations on the model, suggesting areas for future investigation.

250 Although a precise ‘resource’ is not identified, nor is a specific depression signal characterized, multiple  
251 hypotheses suitable for experimental examination can be proposed under healthy and synaptic degenerative  
252 conditions.

- 253 • As described by Oh and colleagues (2015), suppressing the heterosynaptic depression signal could  
254 allow learning driven by potentiation under healthy conditions to continue until resources in the pool(s)  
255 are exhausted. Subsequent learning would require the creation of new resources. As a result, while the  
256 pace of learning may reduce under signal-suppressed conditions compared to when active signals are  
257 present, it would not come to a complete stop until all resources are used with no change in neighboring  
258 spines.
- 259 • Suppression of the depression signal under synaptic degenerative conditions might interfere with  
260 memory retention during synaptic loss if the signal is required for resource replenishment.
- 261 • Excessive activation of the depression signal in both healthy and synaptic degenerative conditions  
262 could result in a temporary surplus of resources that would persist until they are used by potentiating  
263 synapses or degrade over time.
- 264 • A reduction in total resources could hinder learning under healthy conditions, although it would not  
265 stop if vital resources are actively liberated through heterosynaptic depression.
- 266 • A reduction in total resources under synaptic degenerative conditions could accelerate the total loss of  
267 synaptic input and therefore the loss of neuronal/memory activity.
- 268 • In contrast, an increase in available resources might lead to uncontrolled neuronal activity and  
269 potentiation under health conditions.
- 270 • Under conditions of synaptic degeneration, an increase in available resources can contribute to memory  
271 retention.

## CONFLICT OF INTEREST STATEMENT

272 The author declares that the research was conducted in the absence of any commercial or financial  
273 relationships that could be construed as a potential conflict of interest.

## AUTHOR CONTRIBUTIONS

274 JH: Conceptualization, Investigation, Methodology, Software, Visualization, Writing - review & editing

## DATA AVAILABILITY STATEMENT

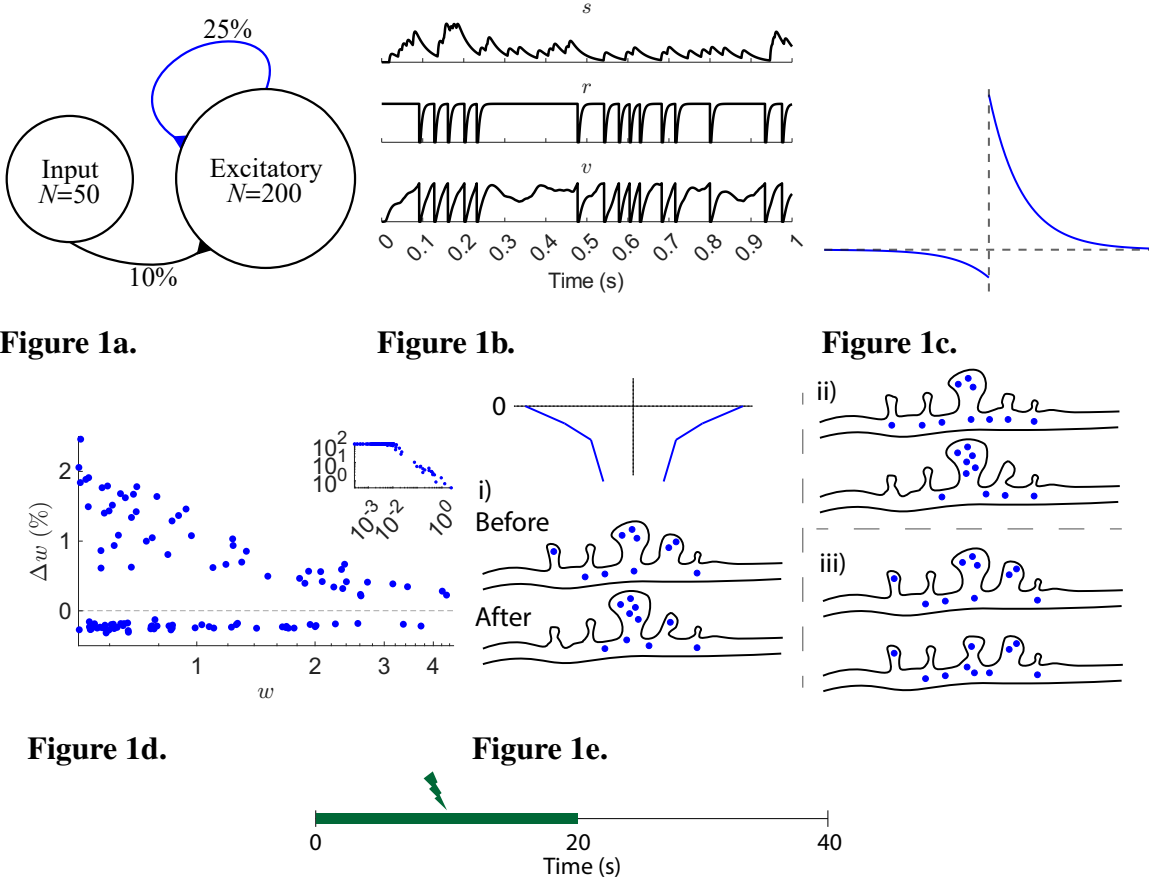
275 The code and datasets generated for this study can be found in GitHub repository.

## REFERENCES

- 276 Abraham, W. C., Logan, B., Greenwood, J. M., and Dragunow, M. (2002). Induction and Experience-  
277 Dependent Consolidation of Stable Long-Term Potentiation Lasting Months in the Hippocampus. *The  
278 Journal of Neuroscience* 22, 9626–9634. doi:10.1523/jneurosci.22-21-09626.2002
- 279 Bannon, N. M., Chistiakova, M., and Volgushev, M. (2020). Synaptic Plasticity in Cortical Inhibitory  
280 Neurons: What Mechanisms May Help to Balance Synaptic Weight Changes? *Frontiers in Cellular  
281 Neuroscience* 14, 204. doi:10.3389/fncel.2020.00204
- 282 Barbour, B., Brunel, N., Hakim, V., and Nadal, J.-P. (2007). What can we learn from synaptic weight  
283 distributions? *Trends in Neurosciences* 30, 622–629. doi:10.1016/j.tins.2007.09.005
- 284 Barnes, S. J., Franzoni, E., Jacobsen, R. I., Erdelyi, F., Szabo, G., Clopath, C., et al. (2017). Deprivation-  
285 Induced Homeostatic Spine Scaling In Vivo Is Localized to Dendritic Branches that Have Undergone  
286 Recent Spine Loss. *Neuron* 96, 871–882.e5. doi:10.1016/j.neuron.2017.09.052
- 287 Bhembre, N., Bonthon, C., and Opazo, P. (2023). Synaptic Compensatory Plasticity in Alzheimer's  
288 Disease. *The Journal of Neuroscience* 43, 6833–6840. doi:10.1523/jneurosci.0379-23.2023
- 289 Bi, G.-q. and Poo, M.-m. (1998). Synaptic Modifications in Cultured Hippocampal Neurons: Dependence  
290 on Spike Timing, Synaptic Strength, and Postsynaptic Cell Type. *The Journal of Neuroscience* 18,  
291 10464–10472. doi:10.1523/jneurosci.18-24-10464.1998
- 292 Bian, W.-J., Miao, W.-Y., He, S.-J., Qiu, Z., and Yu, X. (2015). Coordinated Spine Pruning and  
293 Maturation Mediated by Inter-Spine Competition for Cadherin/Catenin Complexes. *Cell* 162, 808–822.  
294 doi:10.1016/j.cell.2015.07.018
- 295 Billings, G. and Rossum, M. C. W. v. (2009). Memory Retention and Spike-Timing-Dependent Plasticity.  
296 *Journal of Neurophysiology* 101, 2775–2788. doi:10.1152/jn.91007.2008
- 297 Brunel, N., Hakim, V., Isobe, P., Nadal, J.-P., and Barbour, B. (2004). Optimal Information Storage  
298 and the Distribution of Synaptic Weights Perceptron versus Purkinje Cell. *Neuron* 43, 745–757.  
299 doi:10.1016/j.neuron.2004.08.023
- 300 Buzsáki, G. (2004). Large-scale recording of neuronal ensembles. *Nature Neuroscience* 7, 446–451.  
301 doi:10.1038/nn1233
- 302 Buzsáki, G. and Mizuseki, K. (2014). The log-dynamic brain: how skewed distributions affect network  
303 operations. *Nature Reviews Neuroscience* 15, 264–278. doi:10.1038/nrn3687
- 304 Chater, T. E., Eggl, M. F., Goda, Y., and Tchumatchenko, T. (2024). Competitive processes shape  
305 multi-synapse plasticity along dendritic segments. *Nature Communications* 15, 7572. doi:10.1038/  
306 s41467-024-51919-0
- 307 Chater, T. E. and Goda, Y. (2021). My Neighbour Hetero—deconstructing the mechanisms underlying  
308 heterosynaptic plasticity. *Current Opinion in Neurobiology* 67, 106–114. doi:10.1016/j.conb.2020.10.  
309 007
- 310 Chen, J. Y., Lonjers, P., Lee, C., Chistiakova, M., Volgushev, M., and Bazhenov, M. (2013). Heterosynaptic  
311 Plasticity Prevents Runaway Synaptic Dynamics. *Journal of Neuroscience* 33, 15915–15929. doi:10.  
312 1523/jneurosci.5088-12.2013
- 313 Chen, S. and Hillman, D. E. (1982). Plasticity of the parallel Fiber-Purkinje cell synapse by spine takeover  
314 and new synapse formation in the adult rat. *Brain Research* 240, 205–220. doi:10.1016/0006-8993(82)  
315 90217-7
- 316 Choquet, D. and Triller, A. (2003). The role of receptor diffusion in the organization of the postsynaptic  
317 membrane. *Nature Reviews Neuroscience* 4, 251–265. doi:10.1038/nrn1077
- 318 Cooper, L. N. and Bear, M. F. (2012). The BCM theory of synapse modification at 30: interaction of theory  
319 with experiment. *Nature Reviews Neuroscience* 13, 798–810. doi:10.1038/nrn3353

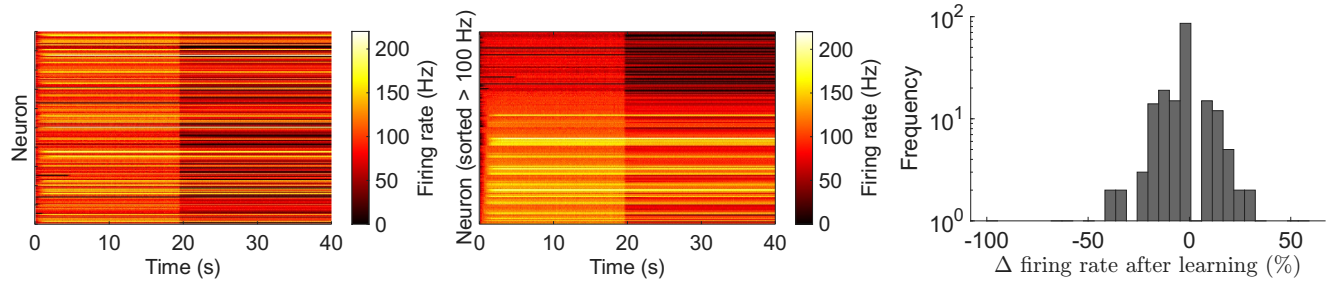
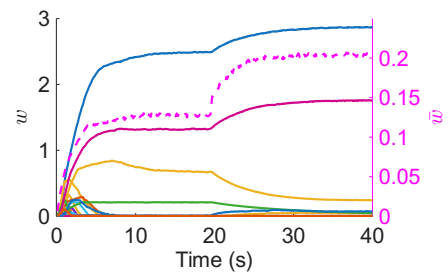
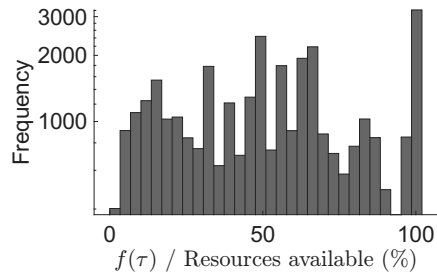
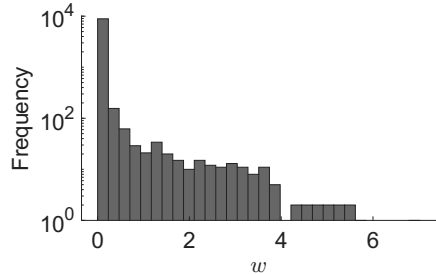
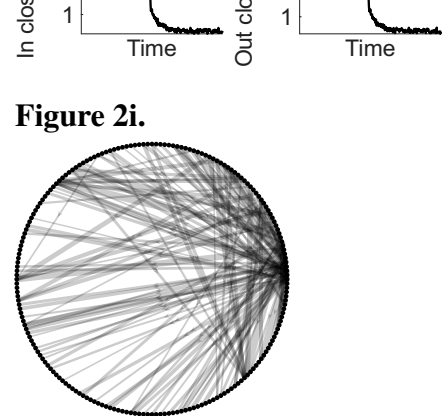
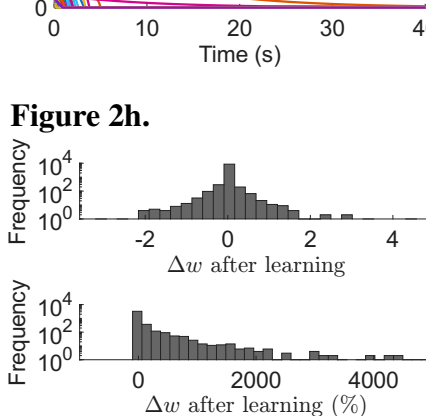
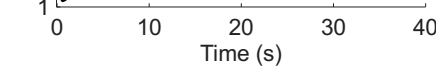
- 320 Debanne, D., Gähwiler, B. H., and Thompson, S. M. (1999). Heterogeneity of Synaptic Plasticity at  
321 Unitary CA3–CA1 and CA3–CA3 Connections in Rat Hippocampal Slice Cultures. *The Journal of*  
322 *Neuroscience* 19, 10664–10671. doi:10.1523/jneurosci.19-24-10664.1999
- 323 Dong, Z., Han, H., Li, H., Bai, Y., Wang, W., Tu, M., et al. (2015). Long-term potentiation decay and  
324 memory loss are mediated by AMPAR endocytosis. *Journal of Clinical Investigation* 125, 234–247.  
325 doi:10.1172/jci77888
- 326 Eckmann, S., Young, E. J., and Gjorgjieva, J. (2024). Synapse-type-specific competitive Hebbian  
327 learning forms functional recurrent networks. *Proceedings of the National Academy of Sciences* 121,  
328 e2305326121. doi:10.1073/pnas.2305326121
- 329 Hayashi, Y., Shi, S.-H., Esteban, J. A., Piccini, A., Poncer, J.-C., and Malinow, R. (2000). Driving AMPA  
330 Receptors into Synapses by LTP and CaMKII: Requirement for GluR1 and PDZ Domain Interaction.  
331 *Science* 287, 2262–2267. doi:10.1126/science.287.5461.2262
- 332 Herms, J. and Dorostkar, M. M. (2015). Dendritic Spine Pathology in Neurodegenerative Diseases. *Annual*  
333 *Review of Pathology: Mechanisms of Disease* 11, 1–30. doi:10.1146/annurev-pathol-012615-044216
- 334 Horton, A. C. and Ehlers, M. D. (2004). Secretory trafficking in neuronal dendrites. *Nature Cell Biology* 6,  
335 585–591. doi:10.1038/ncb0704-585
- 336 Hou, Q., Zhang, D., Jarzylo, L., Huganir, R. L., and Man, H.-Y. (2008). Homeostatic regulation of AMPA  
337 receptor expression at single hippocampal synapses. *Proceedings of the National Academy of Sciences*  
338 105, 775–780. doi:10.1073/pnas.0706447105
- 339 Humble, J. (2013). *Learning, self-organisation and homeostasis in spiking neuron networks using*  
340 *spike-timing dependent plasticity*. Ph.D. thesis
- 341 Humble, J., Hiratsuka, K., Kasai, H., and Toyoizumi, T. (2019). Intrinsic Spine Dynamics Are Critical  
342 for Recurrent Network Learning in Models With and Without Autism Spectrum Disorder. *Frontiers in*  
343 *Computational Neuroscience* 13, 38. doi:10.3389/fncom.2019.00038
- 344 Hunt, S., Leibner, Y., Mertens, E. J., Barros-Zulaica, N., Kanari, L., Heistek, T. S., et al. (2022). Strong and  
345 reliable synaptic communication between pyramidal neurons in adult human cerebral cortex. *Cerebral*  
346 *Cortex* 33, 2857–2878. doi:10.1093/cercor/bhac246
- 347 Kasai, H. (2023). Unraveling the mysteries of dendritic spine dynamics: Five key principles shaping  
348 memory and cognition. *Proceedings of the Japan Academy. Series B, Physical and Biological Sciences*  
349 99, 254–305. doi:10.2183/pjab.99.018
- 350 Kim, H. J., Lee, S., Kim, G. H., Sung, K., Yoo, T., Pyo, J. H., et al. (2025). GluN2B-mediated regulation of  
351 silent synapses for receptor specification and addiction memory. *Experimental & Molecular Medicine*,  
352 1–14doi:10.1038/s12276-025-01399-z
- 353 Korzhova, V., Marinković, P., Njavro, J. R., Goltstein, P. M., Sun, F., Tahirović, S., et al. (2021). Long-term  
354 dynamics of aberrant neuronal activity in awake Alzheimer's disease transgenic mice. *Communications*  
355 *Biology* 4, 1368. doi:10.1038/s42003-021-02884-7
- 356 Lemaréchal, J.-D., Jedynak, M., Trebaul, L., Boyer, A., Tadel, F., Bhattacharjee, M., et al. (2021). A brain  
357 atlas of axonal and synaptic delays based on modelling of cortico-cortical evoked potentials. *Brain* 145,  
358 1653–1667. doi:10.1093/brain/awab362
- 359 Meftah, S. and Gan, J. (2023). Alzheimer's disease as a synaptopathy: Evidence for dysfunction of  
360 synapses during disease progression. *Frontiers in Synaptic Neuroscience* 15, 1129036. doi:10.3389/  
361 fnsyn.2023.1129036
- 362 Montgomery, J. M. and Madison, D. V. (2004). Discrete synaptic states define a major mechanism of  
363 synapse plasticity. *Trends in Neurosciences* 27, 744–750. doi:10.1016/j.tins.2004.10.006

- 364 Morrison, A., Aertsen, A., and Diesmann, M. (2007). Spike-Timing-Dependent Plasticity in Balanced  
365 Random Networks. *Neural Computation* 19, 1437–1467. doi:10.1162/neco.2007.19.6.1437
- 366 Morrison, A., Diesmann, M., and Gerstner, W. (2008). Phenomenological models of synaptic plasticity  
367 based on spike timing. *Biological Cybernetics* 98, 459–478. doi:10.1007/s00422-008-0233-1
- 368 Oh, W., Parajuli, L., and Zito, K. (2015). Heterosynaptic Structural Plasticity on Local Dendritic Segments  
369 of Hippocampal CA1 Neurons. *Cell Reports* 10, 162–169. doi:10.1016/j.celrep.2014.12.016
- 370 Park, M., Penick, E. C., Edwards, J. G., Kauer, J. A., and Ehlers, M. D. (2004). Recycling Endosomes  
371 Supply AMPA Receptors for LTP. *Science* 305, 1972–1975. doi:10.1126/science.1102026
- 372 Penzes, P., Cahill, M. E., Jones, K. A., VanLeeuwen, J.-E., and Woolfrey, K. M. (2011). Dendritic spine  
373 pathology in neuropsychiatric disorders. *Nature Neuroscience* 14, 285–293. doi:10.1038/nn.2741
- 374 Rall, W. (1969). Time Constants and Electrot tonic Length of Membrane Cylinders and Neurons. *Biophysical  
375 Journal* 9, 1483–1508. doi:10.1016/s0006-3495(69)86467-2
- 376 Roche, K. W., O'Brien, R. J., Mammen, A. L., Bernhardt, J., and Huganir, R. L. (1996). Characterization  
377 of Multiple Phosphorylation Sites on the AMPA Receptor GluR1 Subunit. *Neuron* 16, 1179–1188.  
378 doi:10.1016/s0896-6273(00)80144-0
- 379 Rossum, M. C. W. v., Bi, G. Q., and Turrigiano, G. G. (2000). Stable Hebbian Learning from Spike  
380 Timing-Dependent Plasticity. *The Journal of Neuroscience* 20, 8812–8821. doi:10.1523/jneurosci.  
381 20-23-08812.2000
- 382 Royer, S. and Paré, D. (2003). Conservation of total synaptic weight through balanced synaptic depression  
383 and potentiation. *Nature* 422, 518–522. doi:10.1038/nature01530
- 384 Shi, S.-H., Hayashi, Y., Esteban, J. A., and Malinow, R. (2001). Subunit-Specific Rules Governing  
385 AMPA Receptor Trafficking to Synapses in Hippocampal Pyramidal Neurons. *Cell* 105, 331–343.  
386 doi:10.1016/s0092-8674(01)00321-x
- 387 Spires, T. L., Meyer-Luehmann, M., Stern, E. A., McLean, P. J., Skoch, J., Nguyen, P. T., et al. (2005).  
388 Dendritic Spine Abnormalities in Amyloid Precursor Protein Transgenic Mice Demonstrated by Gene  
389 Transfer and Intravital Multiphoton Microscopy. *The Journal of Neuroscience* 25, 7278–7287. doi:10.  
390 1523/jneurosci.1879-05.2005
- 391 Sutton, M. A. and Schuman, E. M. (2006). Dendritic Protein Synthesis, Synaptic Plasticity, and Memory.  
392 *Cell* 127, 49–58. doi:10.1016/j.cell.2006.09.014
- 393 Turrigiano, G. G. (2008). The Self-Tuning Neuron: Synaptic Scaling of Excitatory Synapses. *Cell* 135,  
394 422–435. doi:10.1016/j.cell.2008.10.008
- 395 Washbourne, P., Bennett, J. E., and McAllister, A. K. (2002). Rapid recruitment of NMDA receptor  
396 transport packets to nascent synapses. *Nature Neuroscience* 5, 751–759. doi:10.1038/nn883
- 397 Yasumatsu, N., Matsuzaki, M., Miyazaki, T., Noguchi, J., and Kasai, H. (2008). Principles of Long-Term  
398 Dynamics of Dendritic Spines. *The Journal of Neuroscience* 28, 13592–13608. doi:10.1523/jneurosci.  
399 0603-08.2008

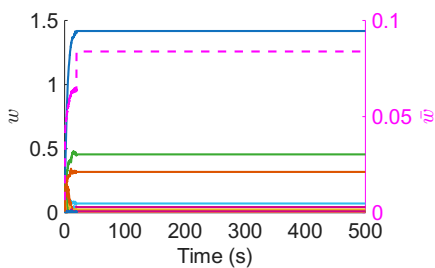


**Figure 1.** Network, neuron, and synaptic models and stimulation protocol. **(A)** A pool of 200 excitatory neurons receive input from 50 independent Poisson processes. All recurrent synapses undergo STDP. **(B)** A synaptic input,  $s$ , and one neuron's refractoriness,  $r$ , and membrane potential,  $v$ . **(C)** STDP learning window. **(D)** Synaptic change dependence on weight. **(E)** Three different scenarios for heterosynaptic plasticity: i) potentiation accompanied by heterosynaptic depression of resources (blue circles) from neighbors, ii) potentiation with resources from the pool, and iii) depression. **(F)** Input is provided for the first 20 s.

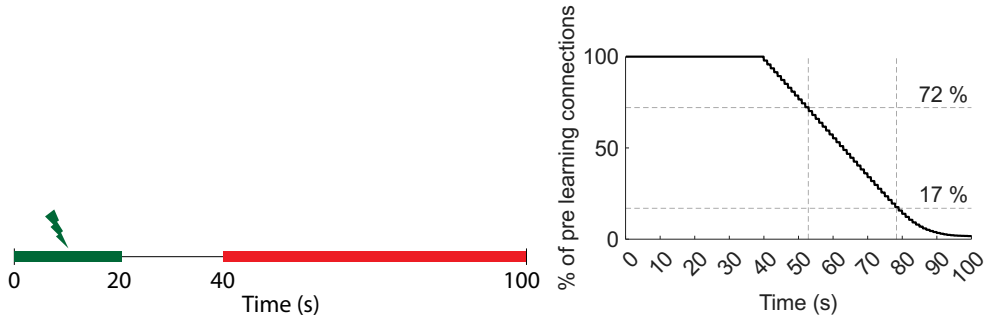
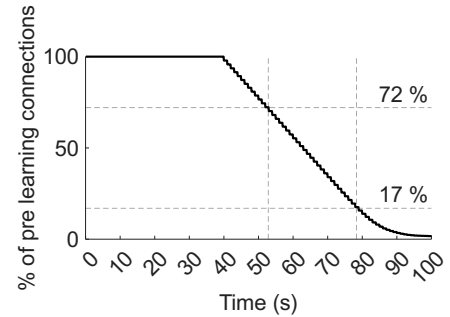
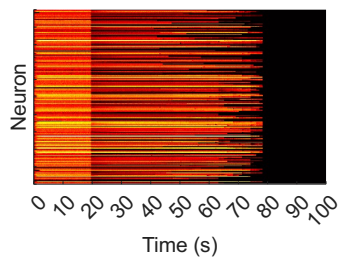
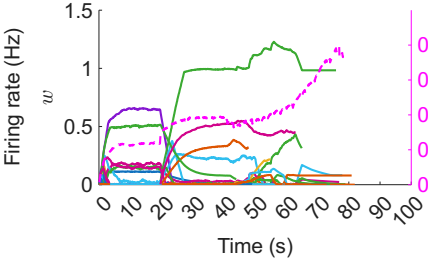
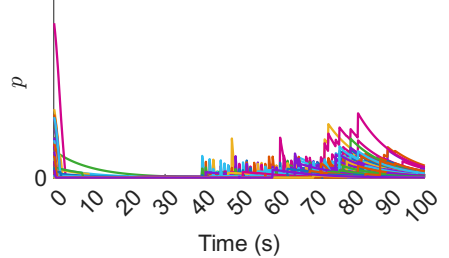
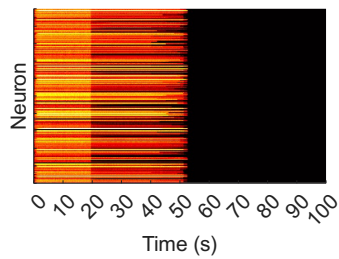
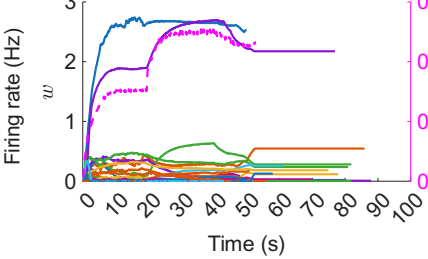
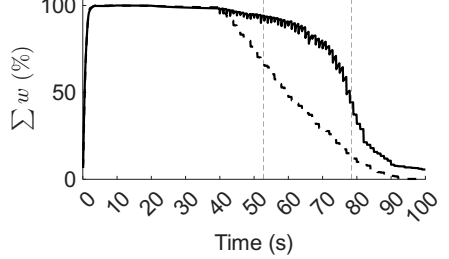
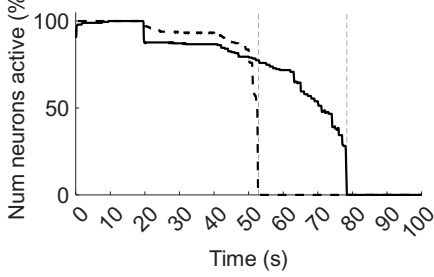
## FIGURE CAPTIONS

**Figure 2a.****Figure 2b.****Figure 2c.****Figure 2d.****Figure 2e.****Figure 2f.****Figure 2g.****Figure 2h.****Figure 2i.****Figure 2j.****Figure 2k.****Figure 2l.**

**Figure 2.** Typical network dynamics. **(A)** Firing rates of the network's neurons. **(B)** Sorted firing rate of the network's neurons for when they first fire  $\geq 100$  Hz. **(C)** Change in the firing rate from after learning to the end of the simulation. **(D)** Weights,  $w$ , at the end of the simulation. **(E)** Actual potentiation amount as a percentage of that determined by the STDP window. **(F)** Left axis: example of 100 synapses' weights. Right axis/dashed line: mean of nonfilopodia synapses' weights. **(G)** Distance between nonfilopodia spines. **(H)** Resource pools,  $p$ . **(I)** Mean in degree, out degree, in closeness, and out closeness during the simulation. **(J)** Network of neurons after learning. **(K)** Weight change after learning. **(L)** Network of neurons at the end of the simulation. **(J)** and **(L)** Only the strongest 10% are shown. Line width represents weight.



**Figure 3.** Left axis: example of 100 synapses' weights during a long simulation. Right axis/dashed line: mean of nonfilopodia synapses' weights.

**Figure 4a.****Figure 4b.****Figure 4c.****Figure 4d.****Figure 4e.****Figure 4f.****Figure 4g.****Figure 4h.****Figure 4i.**

**Figure 4.** Typical network dynamics with and without resource pool replenishment while removing connections. **(A)** Input is provided for the first 20 s. Synapses are progressively deleted from 40 s on (red). **(B)** Progressive synaptic loss. **(C)** Firing rates of the network's neurons with replenishment of the resource pool. **(D)** Left axis: example of 100 synapses' weights with resource pool replenishment. Right axis/dashed line: mean of nonfilopodia synapses' weights. **(E)** Resource pools,  $p$ , with replenishment of the resource pool. **(F)** Firing rates of the network's neurons without replenishment of the resource pool. **(G)** Left axis: example of 100 synapses' weights without replenishment of the resource pool. Right axis/dashed line: mean of nonfilopodia synapses' weights. **(H)** Sum of weights as a percentage of the maximum sum of weights. Solid line, with resource replenishment; dashed line, without resource replenishment. **(I)** The number of active neurons as a percentage of the maximum number of active neurons. Solid line: with resource replenishment; Dashed line: without resource replenishment. **(B), (H), and (I)** Vertical lines are when all neurons stopped firing either with or without resource replenishment. **(D) and (G)** Weights are shown while they exist and the mean of nonfilopodia synapses' weights is shown while neurons are active.